Vertex Group Effects in Entangled Polystyrene−Polyhedral Oligosilsesquioxane (POSS) Copolymers

Jian Wu,[†,§] Timothy S. Haddad,[‡] and Patrick T. Mather*[,†,§]

Polymer Program and Department of Chemical Engineering, University of Connecticut, Storrs, Connecticut 06269, and ERC, Inc., AFRL/PRSM, Edwards Air Force Base, California 93524

Received October 30, 2008; Revised Manuscript Received December 22, 2008

ABSTRACT: The linear viscoelastic behavior of thermoplastic hybrid inorganic−organic polymers synthesized through radical copolymerization of styrene and styryl-based polyhedral oligosilsesquioxane (POSS), $R_7(Si_8O_{12})(C_6H_4CH{=}CH_2)$, with R = isobutyl (^{i}Bu), cyclopentyl (Cp), and cyclohexyl (Cy), was studied to reveal a significant influence of the vertex group, R. The glass transition temperatures were found to feature a strong and complex POSS vertex group dependence, with ^{i}Bu playing a plasticizer-like role and Cp and Cy enhancing the glass transition. Rheological measurements showed that all of the copolymers with lower weight fractions of POSS (0, 6, and 15 wt %) followed the time−temperature superposition (tTS) principle. The rubbery plateau modulus (G_N^0) was found to decrease with increasing POSS content and showed a strong dependence on vertex group, with the ordering ^{i}BuPOSS > CpPOSS > CyPOSS, indicating increasing entanglement dilution with POSS size. At low deformation frequencies, a terminal zone was observed for the ^{i}BuPOSS-based copolymers, like pure PS; however, CpPOSS and CyPOSS copolymers lead to low-frequency elasticity for higher POSS contents, suggesting a weak physical network, with a particular CpPOSS copolymer revealing critical gel behavior. We ascribe the observed rheological data to two distinct effects of POSS incorporation: (i) the effect of POSS grafting on microscopic topology of polymer chains and (ii) intermolecular interaction between POSS and PS chain segments. From Vogel−Tanmman−Fulcher plots of the terminal relaxation time, the apparent activation energy values for each copolymer series were found to monotonically increase with POSS content, indicating that POSS decreases rheological temperature sensitivity, consistent with tTS analysis for free volume thermal expansivity.

Introduction

Polymer scientists actively seek to develop and understand hybrid nanomaterials—composites with a reinforcing phase that has at least one characteristic dimension in the range 1−100 nm—in order to realize materials that combine the processability and property-tuning of polymers with outstanding stiffness and stability (thermal and chemical) of a reinforcing phase.[1−3] To date, an emphasis has been placed on the top-down approach of dispersing nanoscopic fillers within a polymer host with either melt-mixing or solvent-assisted processing, the former being much more desirable for scaling to industrial processes. The most studied reinforcing fillers have been clay (aluminosilicates), graphite, silica, and carbon nanotubes. While few detailed rheological studies have been undertaken, it appears common that the rheological characteristics of the nanocomposite polymer host are adversely affected—from a processing perspective—through significant increases in melt viscosity and the creation of an elastic network with finite yield stress. Another, bottom-up, approach to hybrid nanocomposites involves the copolymerization of a nanoscopic hybrid monomer, POSS, where POSS is a well-defined, chemically functionalized spherosilicate termed polyhedral oligosilsesquioxane. POSS can be incorporated into polymers through chain-growth polymerizations with the use of vinyl- or vinylidene-functionalized POSS (e.g., styryl-POSS[4,5] or methacryl-POSS[6]), step-growth polymerizations of diamino POSS[7] or simple end-capping with monofunctional POSS.[8] In contrast with the previously described dispersion route to hybrid nanocomposites, where nanoscale morphology is determined primarily by mixing and dispersion, the bottom-up approach leads more naturally to good dispersion (molecular scale to nanoscale) that is determined primarily at the polymer synthesis stage and thermodynamically controlled self-assembly of the POSS moieties.[9] However, similar to the dispersion route, rheological properties of POSS-based nanocomposites can be quite distinct from their homopolymer counterparts. Successful processing of POSS-based polymers requires an understanding of such rheological modifications, and this is the subject of our present investigation.

In our previous paper,[5] we demonstrated the essential role of the characteristic nanoscopic size of POSS moieties in determining the rheological properties of PS-based random copolymers incorporating isobutyl-functionalized POSS macromers (^{i}BuPOSS). The incorporation of ^{i}BuPOSS significantly changed the polymer chain topology and introduced additional free volume, resulting in a decrease of glass transition temperature and rubbery plateau modulus but an increase in flow activation energy. Considering its nanoscopic character, POSS macromers feature one functional group and seven inert organic groups (so-called "R groups"), all at the silicon−oxygen polyhedron vertex positions. Here, we will use the terminology "vertex group" in reference to the inert organic "R groups" of POSS macromers and "pendent group" in reference to the entire tethered POSS. On a volumetric basis, and recognizing molecular motion, vertex groups may occupy as much as 80% of the molecular volume,[10] and this volume mediates interaction with other POSS groups and with non-POSS polymeric segments.

Thus far, some published research work has revealed that the vertex group is one of the key factors to control POSS dispersion and the resulting rheological properties. Romo-Uribe et al.[4] reported the linear viscoelastic properties of unentangled random copolymers from 4-methylstyrene and its POSS derivatives with cyclopentyl (Cp) and cyclohexyl (Cy) vertex groups. It was found that with increasing POSS content the pendent CpPOSS and CyPOSS moieties tended to aggregate and form nanocrystals in the polymer matrix. Consequently, the corresponding rheological properties were profoundly altered with

* To whom correspondence should be addressed.
† University of Connecticut.
‡ ERC, Inc.
§ Current address: Syracuse Biomaterials Institute and Biomedical and Chemical Engineering Department, Syracuse University, Syracuse, NY 13244.

10.1021/ma8024267 CCC: $40.75
Published on Web 01/30/2009

Scheme 1. Synthetic Scheme for the Preparation of Random Copolymers Yielded from Styrene and Styryl-POSS through Radical Copolymerization Initiated by AIBN at 60 °C[a]

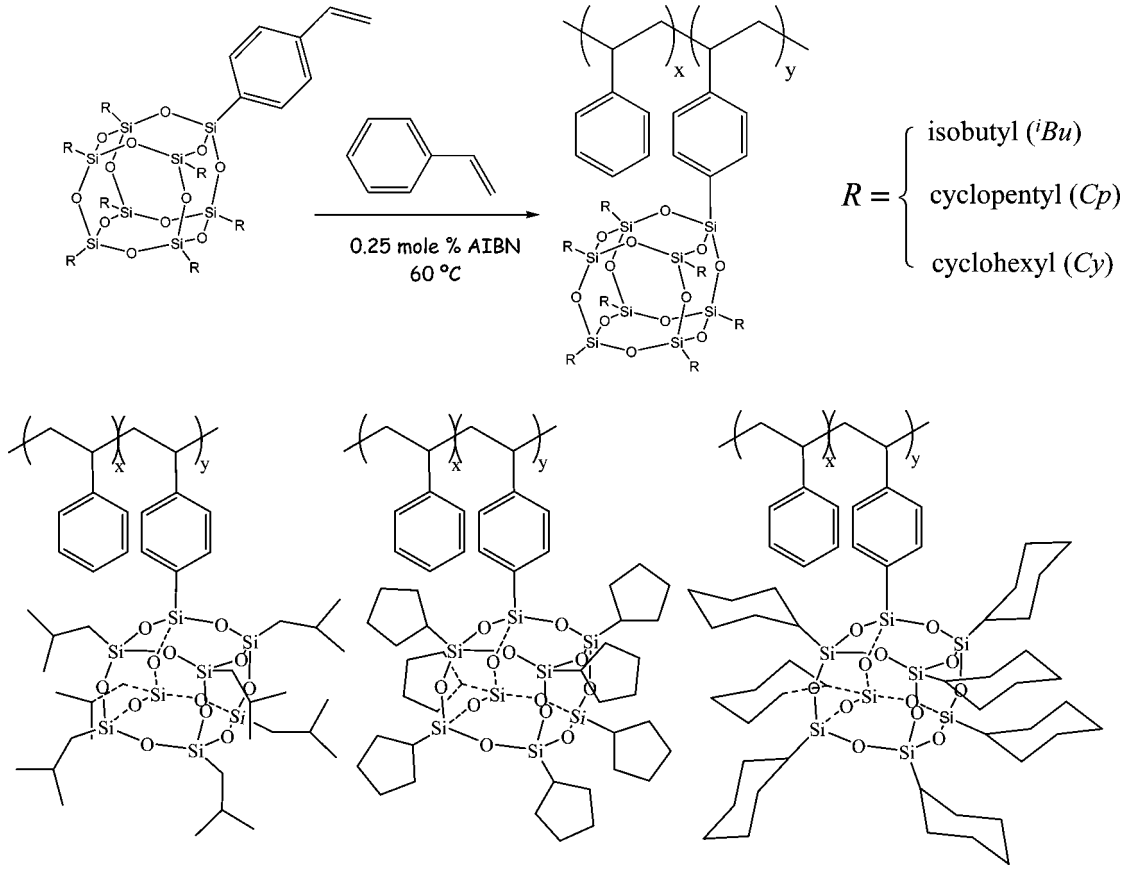

[a] POSS vertex group varies with isobutyl (^{i}Bu), cyclopentyl (Cp), and cyclohexyl (Cy), drawn left to right on the bottom of the scheme.

the increasing POSS incorporation level. Above a critical mole fraction of 8 mol % CyPOSS, a secondary rubbery plateau appears with a magnitude $\sim 10^3$ Pa and in the frequency range where traditional terminal zone behavior occurs for the non-POSS analogue. By comparison, CpPOSS-incorporating copolymers featured a higher critical mole fraction of ~16 mol % for the onset of low-frequency solidlike response. They attributed this phenomenon to the intermolecular interaction due to the presence of POSS and can be described by the "sticky reptation" model developed by Leibler et al.,[11] which was conceived to describe the dynamics of hydrogen-bonded elastomers.[12,13] Unfortunately, because of the limited polymerization degree, findings on the narrow rubbery plateau (and the corresponding entanglement molecular weight) were a result of both molecular weight variation and POSS content, thus making it impossible to clarify an isolated POSS effect.

Kopesky et al.[6] reported the linear viscoelastic properties of poly(methyl methacrylate) (PMMA) tethered and untethered by POSS. They found that the introduction of isobutyl-POSS (^{i}BuPOSS) led to an apparent increase of entanglement molecular weight. Meanwhile, at the same POSS loading (25 wt %), the copolymer with CyPOSS featured a higher plateau modulus than the analogous ^{i}BuPOSS copolymer. To be contrasted with the random copolymers incorporating ^{i}BuPOSS, the terminal behavior of those tethered by CyPOSS showed significant rheological deviation from the expected terminal zone frequency dependence of storage and loss modulus: $G' \sim \omega^2$ and $G'' \sim \omega^1$, where G' and G'' are the shear storage and loss modulus, respectively.[14]

Clearly, the POSS vertex group offers a compositional means to control the rheological behavior of polymers incorporating POSS. However, only a few papers (those discussed above) have reported the rheological behavior of POSS-based polymeric nanocomposites as a function of vertex group in detail. Therefore, we were compelled to systematically explore the vertex group dependence of linear viscoelastic properties in the POSS-tethered polymers. In this paper, we seek to quantitatively reveal the role of vertex group composition in determining the linear viscoelastic properties of polymeric nanocomposites bearing POSS, using polystyrene (PS) as the model polymeric "host" copolymerized to yield POSS-pendent polymers with a variety of vertex groups: isobutyl (^{i}Bu), cyclopentyl (Cp), and cyclohexyl (Cy).

Experimental Section

Materials. In order to quantitatively elucidate vertex group dependence of the linear viscoelastic properties of polymeric nanocomposites bearing POSS moieties, we synthesized a series of PS-based random copolymers in the range of 0−50 wt % POSS macromer loading and with distinct vertex groups, specifically isobutyl (^{i}Bu), cyclopentyl (Cp), and cyclohexyl (Cy). As shown in Scheme 1, the random copolymers were synthesized through free radical copolymerization using methods previously described.[5,15] Briefly, a 10.0 molal monomer solution in toluene containing a total of 3 g of monomers was initiated using 0.25 mol % azobis(isobutyronitrile) (AIBN). One representative synthesis to yield 6 wt % POSS (designated hereafter as $PS_{94}CyPOSS_6$) follows: Under a nitrogen atmosphere, a dry O_2-free solution of toluene (2.73 mL), $[(C_8H_7)Cy_7(Si_8O_{12})]$ (180 mg, 0.196 mmol), styrene (2820 mg, 27.08 mmol), and AIBN (11.2 mg, 0.068 mmol) was heated to 60 °C for 2 days. This was then diluted with 15 mL of $CHCl_3$ and precipitated into 100 mL of methanol. After stirring for 1 h, the copolymer was isolated on fritted glassware and air-dried

overnight. ^{1}H NMR spectroscopy (400 MHz) showed no unreacted monomers and confirmed that the product contained 0.70 mol % or 6 wt % POSS. The isolated yield of dry copolymer was 80% of the theoretical value. Other PS−POSS copolymers were polymerized in an identical fashion and isolated in yields ranging from 76 to 98%. We have adopted a nomenclature to immediately distinguish samples by composition: PS_XRPOSS_Y, where X is the wt % of styryl comonomer, R is the POSS vertex group, and Y is the wt % of POSS comonomer. As one example, PS_{85}[i]$BuPOSS_{15}$ is a random copolymer containing 85 wt % PS and 15 wt % [i]BuPOSS.

We observed that the solubility of the random copolymers prepared from styrene and styryl-POSS depended strongly on the vertex group. The random copolymers incorporating [i]BuPOSS (up to 50 wt % [i]BuPOSS content) readily dissolve in tetrahydrofuran (THF); however, the random copolymers incorporating CpPOSS and CyPOSS cannot dissolve completely in organic solvents (such as THF, toluene, and $CHCl_3$) and can only be swollen when POSS loading is beyond 15 wt % CpPOSS and 30 wt % CyPOSS, respectively. This solubility difference is apparently due to the formation of a physical network by a multitude of POSS−POSS associations; cyclopentyl- and cyclohexyl-POSS have a much stronger degree of affinity than isobutyl-POSS. This effect is not realized in unentangled low degree of polymerization copolymers. Because of this limitation of solubility, we only choose the random copolymers with POSS loading up to 15 wt % to compare the effect of vertex group on the rheological properties of random copolymers bearing POSS. 5 wt % polymer solutions in THF were cast into Teflon casting dishes, 10 cm in diameter, and dried at room temperature for 4 days. Next, the free-standing cast films were dried in vacuum at 50−60 °C for 2 days and then at 80−90 °C for 2 days. In order to remove any residual solvent (THF), the films were finally dried above T_g (∼120 °C) for a further 12 h. The cast films dried in this manner had thicknesses of ∼1.0 mm and were employed for further microstructural and physical characterizations.

Characterization. *Wide-Angle X-ray Scattering (WAXS).* In order to assess the microstructures of the random copolymers, wide-angle X-ray scattering (WAXS) experiments were conducted at room temperature on the samples using a Bruker D5005 X-ray diffractometer with rotating anode source operated at 40 kV and 40 mA. Nickel-filtered Cu Kα radiation with wavelength λ = 1.5418 Å was used as the source. The scattering angle, 2θ, was scanned from 5° to 40° at a rate of 1.0 deg/min.

Nuclear Magnetic Resonance Spectroscopy (NMR). ^{1}H NMR spectra were collected to assess monomer purity, monomer-free polymer, and to confirm the polymer backbone chemical structure. The spectra were obtained in $CDCl_3$ solvent (∼30 mg/mL) using either a Bruker 400 or 300 MHz instrument. Standard 1D proton spectra were obtained using a 30 s delay between pulses to ensure complete relaxation and therefore accurate integral measurements.

Thermal Analysis. The thermal transitions of the random copolymers were characterized using differential scanning calorimetry (DSC), employing a TA Instruments DSC-2920 equipped with a mechanical intercooler (cooling capability to $T = -60$ °C) under a continuous nitrogen purge (50 mL/min). Both calibrations of heat flow and temperature were based on a run in which one standard sample (indium) is heated through its melting point. The samples were sealed in aluminum pans with mass in the range 5−10 mg. All measurements were conducted at a scan rate of 10 °C/min following a heat−cool−heat procedure from 0 to 250 °C. Glass transition temperatures (T_g) were determined by the midpoint of heat flow step-down (heat capacity step up) during second heating. In order to further assess the vertex group influence on the compatibility of POSS in PS host, samples with 50 wt % POSS loading, though insoluble, were annealed at 150 °C for 12 h. After annealing, the samples were quenched to 0 °C and heated up to 250 °C with ramping rate of 10 °C/min in order to investigate their glass transition temperature and melting behavior.

Rheological Measurements. Linear viscoelastic properties were measured using an ARES rheometer (TA Instruments, Inc.). It was equipped with two torque transducers distinguished by their torque capacity: 200 and 2000 g·cm. The existence and extent of the linear viscoelastic regime were determined by measurements of the dynamic storage and loss moduli, $G'(\omega)$ and $G''(\omega)$, as functions of strain (0.1−10%) at an angular frequency with 10 rad/s. All of the measurements were carried out within the linear viscoelastic range, where $G'(\omega)$ and $G''(\omega)$ were independent of strain. The dynamic moduli were measured as a function of frequency over the range 0.01 rad/s < ω < 100 rad/s at various temperatures above T_g in the range 120 °C < T < 180 °C and under a nitrogen atmosphere. All of the rheological characterizations were performed using the parallel plates with 8 mm diameter and with the gap between two plates being about 1.0 mm and known within 1 μm resolution.

Table 1. Summary of Molecular Characteristics of Polystyrene−POSS Copolymers[a,b]

compound	$M_w \times 10^3$ (g/mol)	M_w/M_n	DP	wt % POSS	mol % POSS	no. $POSS_{chain}$
PS_{100}	161	1.43	1080	0.0	0.0	0
PS_{94}[i]$BuPOSS_6$	186	1.46	1165	5.9	0.70	8
PS_{85}[i]$BuPOSS_{15}$	195	1.40	1158	15.4	2.02	23
PS_{67}[i]$BuPOSS_{33}$	300	1.52	1390	33.2	5.34	64
PS_{48}[i]$BuPOSS_{52}$	419	1.65	1358	52.1	10.95	138
$PS_{94}CpPOSS_6$	235	1.70	1248	6.1	0.66	8
$PS_{85}CpPOSS_{15}$	436	2.53	1410	15.3	1.80	25
$PS_{70}CpPOSS_{30}$	insoluble					
$PS_{50}CpPOSS_{50}$	insoluble					
$PS_{94}CyPOSS_6$	191	1.77	982	6.1	0.60	6
$PS_{85}CyPOSS_{15}$	294	2.07	1180	15.2	1.64	19
$PS_{70}CyPOSS_{30}$	635	2.81	1582	30.4	3.89	62
$PS_{50}CyPOSS_{50}$	insoluble					

[a] Molecular weight and molecular weight distribution were determined by gel permeation chromatography (GPC) in $CHCl_3$, calibrated by polystyrene (PS) standards. [b] DP's are calculated from M_n and wt % POSS is derived from mol % POSS, which is directly measured from ^{1}H NMR spectroscopy.[16]

Results

Synthesis and Characterization of PS−POSS Copolymers. A series of PS-based random copolymers bearing POSS moieties with varying vertex group composition were synthesized by free radical polymerization in the presence of azobis(isobutyronitrile) (AIBN) as a radical initiator. GPC results revealed that all of the polymers synthesized were characterized by high molecular weight ($M_w > 1.5 \times 10^5$ g/mol) and correspondingly high number-average polymerization degree (DP > 1000). Their polydispersity indices (PDI) were typical of free radical polymerization, e.g., PDI > 1.4, and showed notable vertex dependence. Specifically, at high POSS loading, the copolymers bearing [i]BuPOSS feature lower PDI values than the counterparts bearing CpPOSS and CyPOSS. Furthermore, PDI values of the latter copolymers increased with increasing CpPOSS and CyPOSS loading, which could be due to their decreasing solubility with increasing CpPOSS and CyPOSS incorporation in the reaction media, toluene. ^{1}H NMR characterization revealed that the actual POSS incorporation ratio in copolymers was very close to the feeding ratio and independent of vertex group. These observations indicate that styryl-POSS macromer has very similar reactivity to that of styrene monomer and that the pendent POSS group does not influence the reactivity of the covalently attached styryl for free radical polymerization. The molecular characteristics of the copolymers are detailed in Table 1.

Microstructure. Figure 1 shows the wide-angle X-ray scattering (WAXS) patterns of the three styryl-POSS macromers and PS-based random copolymers incorporating POSS moieties with three kinds of vertex groups ([i]Bu, Cp, and Cy), all taken at room temperature. As shown in Figure 1a, all three styryl-POSS macromers feature the very intense and sharp diffraction peaks associated with the macromer crystalline structures. The single strongest characteristic diffraction peaks of POSS mac-

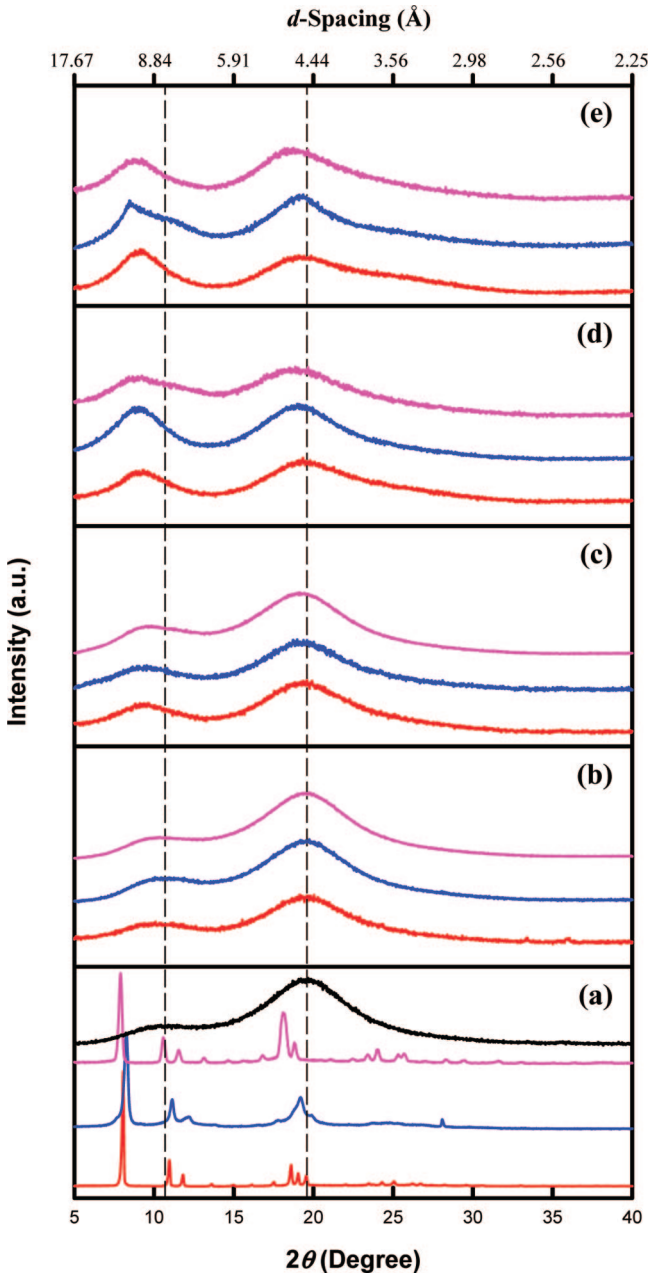

Figure 1. WAXS patterns of PS-based random copolymers with varying POSS vertex group and POSS loading level. (a) Pure POSS macromers and neat PS. Red, blue, and pink solid lines represent iBuPOSS, CpPOSS, and CyPOSS macromers, respectively. Black solid line stands for pure PS. The weight percentage of POSS loading level varies with (b) 6, (c) 15, (d) 30, and (e) 50 wt % POSS. Red, blue, and pink solid lines represent iBuPOSS-, CpPOSS-, and CyPOSS-based random copolymers, respectively. The two black dash reference lines represent the characteristic scattering peak of pure PS centered at *d*-spacing of 4.5 and 8.3 Å.

romers with isobutyl (^{i}Bu), cyclopentyl (Cp), and cyclohexyl (Cy) are centered at *d*-spacing of 11.0, 10.8, and 11.2 Å, respectively. The WAXS pattern of pure PS is characterized by two amorphous halos: one is centered at a *d*-spacing of 4.5 Å, ascribed to the correlation length between benzene rings along the chains,[17] and the other is centered at 8.3 Å, attributed to the interchain correlation distance.[18] WAXS patterns of the copolymers bearing POSS were found to be quite similar to each other, despite their differing vertex groups. All of them lack crystalline diffraction peaks of the POSS macromer crystals and, instead, indicate very similar structure to amorphous PS. In particular, for all of the copolymers studied, two characteristic amorphous halos appear, representing the interchain correlations at lower 2θ angle and the correlation distance between side groups along the chains at higher 2θ angle.

At the lower POSS loading level (≤30 wt %), WAXS patterns of copolymers feature similar trends with increasing of POSS content among the different POSS vertex groups: the amorphous halo at the *d*-spacing = 8.3 Å shifts to lower scattering angles, and the corresponding peak is slightly narrowed. Meanwhile, the amorphous halo at the *d*-spacing = 4.5 Å becomes a little broadened and also shifts to lower scattering angles. That the characteristic scattering peaks shift to larger *d*-spacing means that the incorporation of POSS moieties enlarges the interchain correlation distance and inter-side-group correlation.[5] Furthermore, in contrast with the styryl-POSS macromers, these two peaks are quite distinct from any crystalline reflections of the corresponding styryl-POSS macromers. In particular, the strongest ^{i}BuPOSS macromer reflections appear at *d*-spacings of 11.0 and 8.1 Å; however, these regions of the copolymer WAXD patterns are devoid of any features. Thus, it is clear that copolymerization effectively prevents crystallization (or even aggregation) of POSS units, at least for low POSS contents (≤30 wt %). That said, WAXS data alone cannot distinguish the existence of small POSS clusters (2−3 molecules) or not.

Compared with the samples containing 30 wt % POSS, the copolymer incorporating 50 wt % CpPOSS ($PS_{50}CpPOSS_{50}$) exhibits a sharp peak centered at *d*-spacing = 10.5 Å, which is very close to the strongest diffraction peak of styryl-CpPOSS macromer. Further, copolymers incorporating 50 wt % ^{i}BuPOSS ($PS_{50}{}^{i}BuPOSS_{50}$) and 50 wt % CyPOSS ($PS_{50}CyPOSS_{50}$) exhibit only further narrowing of the diffuse scattering peak at higher *d*-spacing (lower 2θ)—remaining diffuse—and shifting of the smaller *d*-spacing halo (interchain spacing) to larger *d*-spacing. This stands in contrast to $PS_{50}CpPOSS_{50}$, which exhibited a crystalline diffraction peak at low angle. These distinct features at higher *d*-spacing provide evidence that the compatibility between POSS moiety and PS host has a vertex group dependence: CpPOSS is less compatible with the PS host than ^{i}BuPOSS and CyPOSS. The lack of microscopic ^{i}BuPOSS and CyPOSS aggregation in PS host may be due to the favorable interaction between POSS moieties and the PS segments, at least in comparison to POSS−POSS and PS−PS segmental interactions.

Indeed, prior research has indicated preferential interactions of POSS with polymer segments. Zhang et al.[19] studied the effect of random copolymers of PMMA−POSS on the phase segregation of the typical immiscible polymer blend of PMMA and PS prepared from spin-coating of toluene solution. They found that the CpPOSS moieties pendent to PMMA compatibilized polymer blends of PMMA and PS, indicated by profound interfacial tension reduction and interfacial fracture toughness increase. The authors attributed their observations to a favorable interaction between CpPOSS and PS homopolymer, combined with POSS attachment to a PMMA backbone that maintained the copolymers at the PS/PMMA interface. In the present study, comparison of CpPOSS, ^{i}BuPOSS, and CyPOSS systems using WAXS analysis revealed that isobutyl-POSS (^{i}BuPOSS) and cyclohexyl-POSS (CyPOSS) featured a stronger favorable interaction with the PS host than CpPOSS, which aggregates to form nanocrystals in PS host when CpPOSS loading is beyond a critical concentration.

We must emphasize that at the lower POSS contents used in rheological investigations, in particular ≤15 wt %, the vertex group dependency of the apparent compatibility between POSS and PS host does not significantly influence the microstructure of the copolymers as revealed in WAXS pattern similarity. Regardless of vertex group, the pendent POSS groups are dispersed in the PS matrix nearly at a molecular level for these

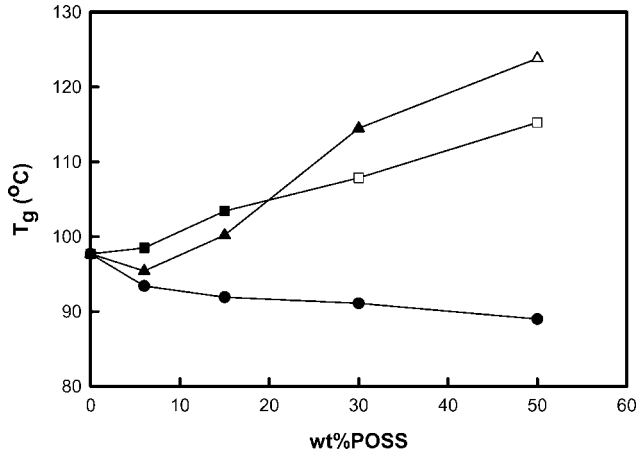

Figure 2. Variation of glass transition temperature (T_g) for as-cast PS-based copolymers films as the function of POSS content. T_g is determined from the midpoint of enthalpy change in the DSC trace curves. POSS vertex group varies with (●) ^{i}BuPOSS, (■) CpPOSS, and (▲) CyPOSS. The open symbols represent the samples insoluble.

cases. Despite the microstructural similarity observed with WAXS, we anticipated vertex group specificity in physical property determination, given prior findings[4] and POSS/styrene−segment interaction differences implied by WAXS at higher loadings. As such, the corresponding thermal and rheological properties are discussed in the following several sections.

Thermal Transitions. The effects of POSS vertex group composition and POSS incorporation level on glass transition temperatures (T_g's) of the PS-based random copolymers were measured using differential scanning calorimetry (DSC). The glass transition temperatures determined from the midpoint of enthalpy change are shown in Figure 2 (DSC curves are supplied in Supporting Information, Figure 2). As can be observed, the glass transition temperatures of the random copolymers depend in a complex way on POSS loading level and vertex group. First, we investigated the effect of POSS content. For ^{i}BuPOSS-containing copolymers, the glass transition monotonically decreases with the increase of POSS loading, while the random copolymers bearing CpPOSS show the *opposite* trend: T_g increases with increasing CpPOSS content. CyPOSS-containing copolymers show intermediate behavior with nonmonotonic composition dependence, in particular a minimum value of glass transition between 0 and 15 wt % POSS loading. Thus, the glass transition temperature of pure PS is higher than that of copolymer incorporating 6 wt % CyPOSS but lower than that of the one incorporating 15 wt % CyPOSS. Beyond 6 wt %, the glass transition temperatures of CyPOSS copolymers increase significantly with CyPOSS loading such that, above 30 wt %, T_g is greater for CyPOSS copolymers than for CpPOSS copolymers.

To understand the observed T_g trends, consider that the presence of side groups is known to influence a particular polymer's T_g by an amount (and in a direction) that depends on the flexibility and bulk of the side group. Usually, rigid side chains and/or pendent groups decrease the flexibility of the backbone chain and lead to an increase in glass transition temperature. In principle, the glass transition of carbon-backbone polymers reflects the rotational energy barriers about σ bonds of the backbone chain, lower glass transition temperatures resulting from lower energy barriers. While rigid side groups may restrict torsion about σ bonds in the backbone chain, increasing T_g, the dominating effect of flexible side groups is to increase free volume, lowering T_g. For example, the glass transition temperatures for the poly(*n*-alkyl methacrylate) family[20] decrease monotonically with the $-(CH_2)_n-CH_3$ side-chain length. In the case of pendent POSS moieties, the combined influence of these competing factors leads to complex T_g dependence on composition.

While POSS cages are undoubtedly rigid and their significant volume can induce a steric barrier that would increase T_g, the high density of chain ends from each dynamic vertex group of POSS is expected to increase free volume, potentially lowering T_g by internal plasticization. Because the size of POSS units (see Figure 1) and overall side-group flexibility are quite similar among the vertex groups (^{i}Bu, Cy, and Cp), we cannot attribute the dramatic and complex vertex group dependence of T_g only on these two competing effects.

Strong specific intermolecular interactions (also called supplementary valences), such as hydrogen bonding, ion−ion interactions, acid−base interactions, among others, can restrict polymer chain motion and result in enhancement of T_g. In our case, the intermolecular interactions between POSS−POSS and POSS−polymer matrix are mainly through van der Waals attraction, which is much weaker than those listed above. However, on a volumetric basis, seven inert vertex groups may contribute 80% of the POSS volume, which mediates interaction between POSS group and non-POSS polymeric segments. Undoubtedly, this kind of van der Waals interaction can be tuned by varying the type of vertex group. In one report, Xu et al.[21,22] found that the presence of styrylisobutyl-POSS made the glass transition of the poly(acetoxystyrene) (PAS) and poly(vinylpyrrolidone) (PVP) decrease dramatically. Once the hydroxylstyrene repeat unit was introduced to these two polymer chains, the glass transition temperatures dramatically increased because of the formation of hydrogen bonds between phenol group and POSS cage oxygens as well as between phenol group and pyrrolidone group. Conversely, for POSS functionalized with cyclopentyl (Cp) and cyclohexyl (Cy) vertex groups, the increase of glass transitions was observed extensively in the random copolymers, such as poly(4-methylstyrene-POSS),[23,24] poly(norbornyl-POSS),[25] poly(methacrylate-POSS),[26] poly(siloxane-POSS),[27] among others. Typically, this takes place with high wt % POSS and is a measure of the interference of a POSS-based physical network with chain motion.

In total, the variation of glass transition temperature in the random copolymers is the net result of several effects: free volume fraction, steric barrier, and POSS−polymeric segment interactions. For ^{i}BuPOSS copolymers, we observed monotonic decrease in T_g with increasing loading (Figure 2) and thus deduce that POSS−segment interactions are dominated by the internal plasticization of local free volume addition. In contrast, it is apparent from Figure 2 that intermolecular POSS−PS segment interactions are important in determining T_g of the CpPOSS and CyPOSS copolymers, with competition between free volume and intermolecular interactions evidenced in the latter case. Additional evidence for noncovalent intermolecular interactions will be found in the rheological behavior above T_g for the same materials, discussed later.

In the last section, we observed a relatively sharp peak in the WAXS pattern of $PS_{50}CpPOSS_{50}$, close to the characteristic diffraction peak of styryl-CpPOSS macromer. To further confirm the presence of nanocrystals formed by POSS aggregation, we annealed the copolymers with 50 wt % POSS at 150 °C for 12 h. The DSC heating curves (see Supporting Information Figure 2) showed that only the $PS_{50}CpPOSS_{50}$ sample featured any evidence of a weak melting peak (T_m = 183.8 °C), which further proves that the tethered CpPOSS moieties can aggregate to form nanocrystals in PS host. Meanwhile, neither $PS_{50}^{i}BuPOSS_{50}$ nor $PS_{50}CyPOSS_{50}$ showed any evidence for POSS crystallization either by WAXS or DSC analysis. Thus,

we are confident that CpPOSS features less compatibility than ^{i}BuPOSS and CyPOSS in the PS host. Although CpPOSS shows phase separation at the nanoscale while CyPOSS does not, it is interesting that the latter features the larger T_g increment than the former. We suggest that the interactions between CyPOSS and PS segments are stronger than those between CpPOSS and the PS host and/or even than between CpPOSS and CpPOSS.

Rheological Behavior. *Time−Temperature Superposition.* To examine the effects of POSS moieties and their vertex groups on the linear viscoelastic properties of PS random copolymers, isothermal frequency sweep tests were conducted within the temperature range 120 °C < T < 180 °C. This limited temperature span was chosen to avoid significant thermal degradation and side reactions, yet features samples compliant enough (as 8 mm disks) to not overtorque the instrument. The principle of time−temperature superposition (tTS) was applied to obtain linear viscoelastic master curves. Frequency sweep data for a range of temperatures were shifted to a common reference temperature of 120 °C, using temperature-dependent frequency shift factors (a_T). The modulus shift factor (b_T) usually is close to unity and was not required here for good superposition.

Figures 3 and 4 compare the master curves of random copolymers with 6 and 15 wt % POSS varying with vertex group, respectively, wherein the data extend over ~8 decades of reduced frequency. Like pure amorphous PS, all of the random copolymers were thermorheologically "simple", allowing time−temperature superposition (tTS) to function within the temperature range, and exhibited glass−rubber transition, a rubbery plateau, and rubber−liquid transition and terminal zone regimes with the decrease of reduced frequency. Thus, all samples studied are entangled as anticipated based on the molecular weight detailed in Table 1.

The time−temperature superposition (tTS) shift factor, $a_T(T)$, can be described by the WLF equation

$$\log a_T = \frac{-C_1^{\mathrm{r}}(T - T_{\mathrm{r}})}{C_2^{\mathrm{r}} + (T - T_{\mathrm{r}})} \tag{1}$$

where $C_1^{\mathrm{r}} = B/2.303f_{\mathrm{r}}$, $C_2^{\mathrm{r}} = f_{\mathrm{r}}/\alpha_{\mathrm{f}}$, and f_{r} is the fractional free volume at the reference temperature T_{r}. Furthermore, plots of $1/\log(a_T)$ vs $1/(T - T_{\mathrm{r}})$ should be linear if the WLF equation is a good representation of the temperature-dependent viscoelastic properties. In such cases, the WLF parameters can be determined from the slopes and intercepts of the plots.[5]

WLF plots of random copolymers with 6 and 15 wt % POSS at reference temperature 120 °C (see Supporting Information Figures 3a,b) reveal the linearity, and thus WLF applicability, for all vertex groups at these loadings. From the slope and intercept, we evaluated the C_1^{r}, C_2^{r}, and f_{r}, whose values at the glass transition temperature can be calculated as described previously.[5] The calculated values of free volume parameters of random copolymers with different POSS content and vertex group are tabulated in Table 2. While a clear trend in fractional free volume with POSS is absent for a fixed reference temperature of 120 °C, employing T_g as the reference temperature reveals an intriguing trend that the reference fractional free volume (f_g) monotonically *increases* with POSS content, regardless of vertex group. (Gratifyingly, the value of f_g for PS (0.0283) is nearly identical to the value reported in the literature.[28]) These results imply that the presence of POSS molecules tends to create void volume in the glassy and melt states, which may increase segmental mobility. Meanwhile, the increase in f_g/B (free volume at T_g) also has a strong dependence on vertex group following the sequence: ^{i}BuPOSS < CyPOSS < CpPOSS. Considering the glass transition behavior discussed previously (Figure 2), it is quite surprising that T_g follows the same trend as f_g/B (at least for low POSS contents), so that the polymer with highest T_g also has highest f_g/B.

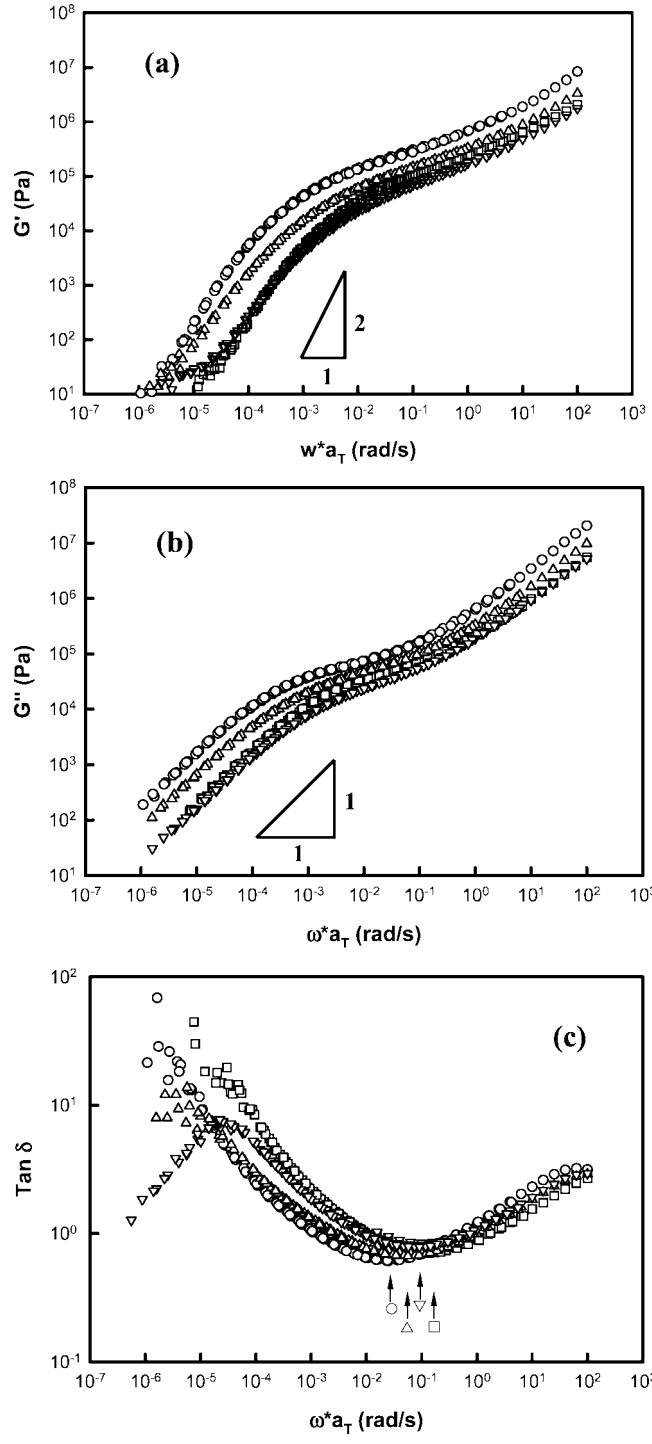

Figure 3. Master curve of the copolymers incorporating 6 wt % POSS varying with vertex group: (○) PS, (□) ^{i}BuPOSS, (△) CpPOSS, (▽) CyPOSS, with reference temperature 120 °C: (a) G', (b) G'', and (c) tan δ. The arrows in (c) indicate the minimum values of tan δ for each sample.

Like the fractional free volume, f_g, α_f also features a strong dependence of POSS loading level and vertex group composition. Regardless of vertex group, the values of α_f *decrease* with increasing POSS content, indicating that the presence of POSS reduces the temperature dependence of fractional free volume. The vertex group dependence of α_f follows the sequence CyPOSS < CpPOSS < ^{i}BuPOSS or inversely with POSS

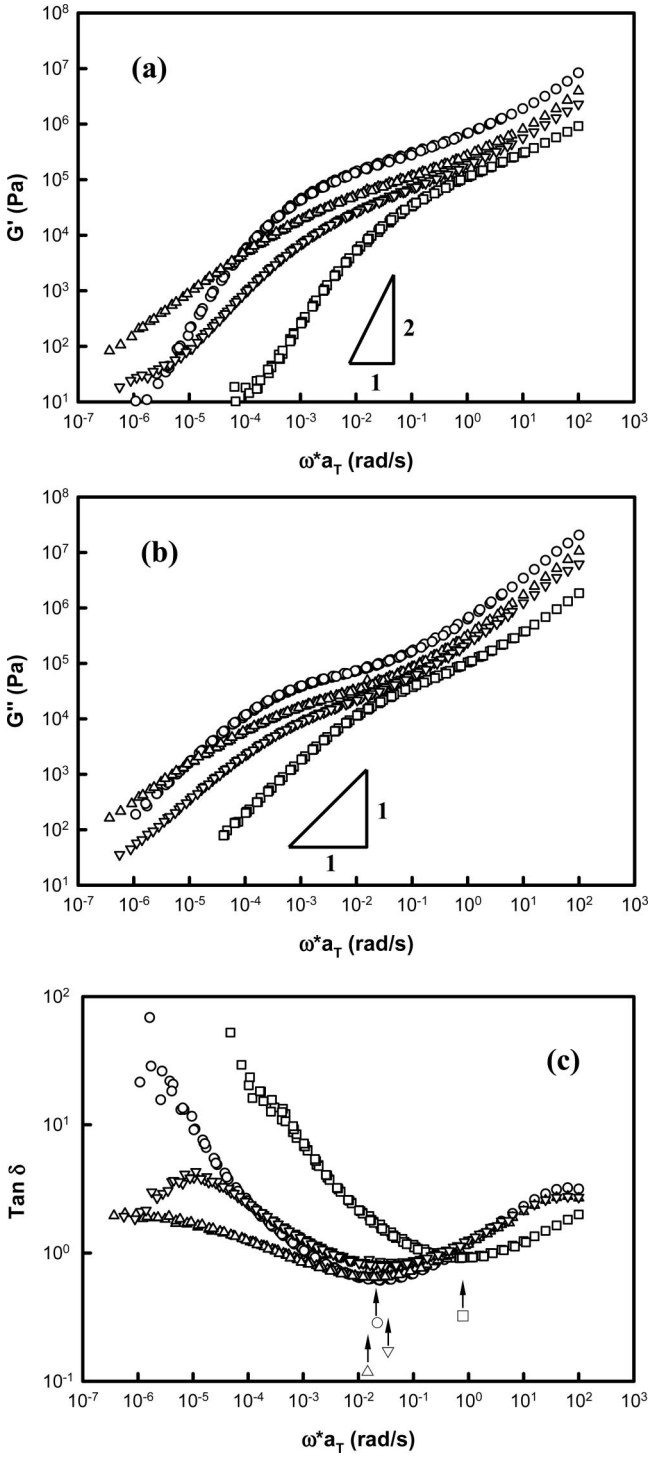

Figure 4. Master curve of the copolymers incorporating 15 wt % POSS varying with vertex group: (○) PS, (□) ^{i}BuPOSS, (△) CpPOSS, (▽) CyPOSS, with reference temperature 120 °C: (a) G', (b) G'', and (c) tan δ. The arrows in (c) indicate the minimum values of tan δ for each sample.

volume.[29,30] Above T_g, fractional free volume f follows the temperature dependence

$$f(T) = f_g + \alpha_f(T - T_g) \qquad T \geq T_g \tag{2}$$

Based on our shift-factor measurements (Table 2), pure PS features much larger $f(T)$ values within the regime of rheological characterization (120 °C < T < 180 °C) than random copolymers incorporating POSS due to its largest α_f value (see Supporting Information Figure 4), although it shows the lowest free volume fraction at T_g. The observed differences suggest that POSS copolymers may exhibit quite lower thermal expansion coefficients than the homopolymer counterparts in the melt, and thus precision molding of amorphous plastics with low residual stress, with CyPOSS-containing systems being the lowest. However, such experiments have not yet been pursued to our knowledge.

Table 2. Summary of Viscoelastic Characteristics of Polystyrene−POSS Copolymers with Various Vertex Group at Reference Temperature 120 °C

compound	C_1^r	C_2^r (K)	f_r/B	f_g/B	α_f (K^{-1})
PS_{100}	8.18	47.84	0.0531	0.0283	11.09×10^{-4}
PS_{94}-^{i}$BuPOSS_6$	8.05	60.10	0.0540	0.0298	8.98×10^{-4}
PS_{94}-$CpPOSS_6$	8.47	57.93	0.0513	0.0323	8.85×10^{-4}
PS_{94}-$CyPOSS_6$	8.51	58.31	0.0510	0.0297	8.75×10^{-4}
PS_{85}-^{i}$BuPOSS_{15}$	9.15	85.55	0.0475	0.0319	5.55×10^{-4}
PS_{85}-$CpPOSS_{15}$	10.06	81.31	0.0432	0.0342	5.31×10^{-4}
PS_{85}-$CyPOSS_{15}$	10.72	96.96	0.0405	0.0323	4.18×10^{-4}

Rubbery Plateau. Rheologically, the so-called rubbery plateau appears above the glass transition temperature[28] and is characterized by the plateau modulus, G_N^0, which is inversely proportional to the average molecular weight between two entanglements (temporary cross-links), termed the entanglement molecular weight, M_e. For polydisperse systems, the plateau modulus can best be determined by applying "tan δ minimum criterion": G_N^0 is equal to the storage modulus G' at the frequency where loss tangent, tan δ, is minimum in the plateau zone[31,32]

$$G_N^0 = |G'|_{\tan\delta \to \min} \tag{3}$$

Indeed, Figures 3c and 4c revealed a well-defined minimum in tan δ for all samples, thus enabling application of this method to the present polydisperse copolymers. Figure 5 shows the plateau moduli of the random copolymers varying with POSS loading and vertex group, revealing monotonic decreases with POSS incorporation levels for all POSS types. The G_N^0 (≈2.0 × 10^5 Pa) of PS we determined in this manner is quite close to the value of plateau modulus obtained by integrating the area under the terminal loss peak of monodispersed entangled PS (1.99 × 10^5 Pa).[28] Meanwhile, G_N^0 is also sensitive to vertex group: the random copolymers incorporating ^{i}BuPOSS show the largest plateau modulus among the various materials and those with CyPOSS feature the lowest G_N^0 values.

The relationship between the characteristic value of G_N^0 and M_e can be expressed as follows:

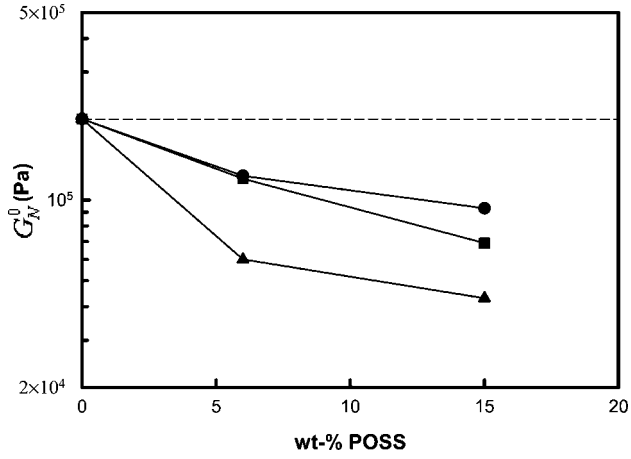

Figure 5. Rubbery plateau modulus (G_N^0) for as-cast films of the random copolymers varying with weight percentage of POSS as a function of vertex group: (●) ^{i}BuPOSS, (■) CpPOSS, (▲) CyPOSS. G_N^0 is determined by G' at minimum tan δ. The dash reference line is plateau modulus of PS reported by Onogi et al. [*Macromolecules* **1970**, *3*, 109−116].

$$G_N^0 = \frac{K\rho RT}{M_e} \quad (4)$$

where R is the universal gas constant, ρ is density, and T is the absolute temperature. K is a constant defined to be 4/5,[33−35] and the density of PS at room temperature is 1.05 g/cm^3. Barry[36] and Larsson[37,38] reported crystal densities of POSS-related molecules with different vertex groups from CH_3- (1.51 g/cm^3) to n-C_4H_9- (1.14 g/cm^3) to 1-naphthyl- (1.24 g/cm^3). All of them have densities higher than PS at room temperature. Qualitatively, it is reasonable to predict that the densities of POSS copolymers are higher than pure PS, though such data are absent from the literature. Therefore, in employing eq 4, we approximated the copolymer density values by utilizing the PS temperature-dependent density, known to follow[39]

$$\rho\ (\mathrm{g/cm^3}) = 1.0865 - 6.19 \times 10^{-4}T + 0.136 \times 10^{-6}T^2; \quad T\ (^\circ\mathrm{C}) \quad (5)$$

for the temperature range 100 °C < T < 220 °C. Using this expression, it is apparent that the density of pure PS decreases slightly from 1.01 to 0.979 g/cm^3 as the temperature increases from 120 to 180 °C. Moreover, melt densities are not expected to increase more than several percent between samples, while G_N^0 values were observed to change nearly an order of magnitude. Thus, dramatic reduction in G_N^0 upon POSS copolymerization implies significant increases in M_e with increasing POSS volume, as shown by the ordering in Figure 5.

Behavior in the Terminal Zone. Within the terminal zone, linear polymer chains fully relax stress by molecular diffusion, leading to the following the characteristic power laws: $G' \sim \omega^2$ and $G'' \sim \omega^1$.[14,35] For the PS−POSS copolymers under study, as shown in Figures 3 and 4, we found the terminal frequency dependence of G'' to feature an exponent close to 1 for all samples, while the frequency dependence of G' at low frequencies revealed a power-law exponent that deviated from 2 significantly and further featured strong vertex group dependence. For random copolymers incorporating ^{i}BuPOSS, the terminal slope of G' (Figures 3a and 4a) is slightly smaller than 2. In contrast, CpPOSS and CyPOSS copolymers featured dramatically altered frequency dependences of storage modulus (G') and loss tangent (tan δ) relative to PS and ^{i}BuPOSS−PS in the terminal regime. For low CpPOSS incorporation levels, $PS_{94}CpPOSS_6$, the terminal behavior is very close to pure PS and the random copolymers incorporating ^{i}BuPOSS. When the CpPOSS content increases to 15 wt %, however, the slope of the resulting loss tangent, tan δ, becomes nearly frequency-independent at a value of ∼2 (Figure 4c; triangles), indicating that G' becomes parallel to G'' for reduced frequencies lower than the crossover of G' and G''. This rheological phenomenon usually appears at the critical condition from liquidlike to solidlike behavior, or so-called "gel point", first described in detail by Winter et al.[40,41] Critical gel behavior for $PS_{85}CpPOSS_{15}$—while surprising—will be further substantiated by relaxation moduli measurements, reported below.

Random copolymers incorporating 6 and 15 wt % CyPOSS also featured nonterminal rheological behavior: at frequencies lower than the crossover of G' and G'', the G' slope decreases with decreasing reduced frequency (showing upward curvature) and tends toward frequency independence. This results in a clear tan δ peak and a secondary G' plateau, as shown in Figures 3c and 4c and Figures 3a and 4a, respectively, each at low frequencies. With increasing CyPOSS loading levels, this secondary G' plateau increases. It is evident that no real terminal zone is exhibited in the random CyPOSS copolymers incorporating. By comparison, as discussed above, $PS_{85}CpPOSS_{15}$ showed critical gelation behavior, a regime perfectly intermediate between liquid and solid, while 6 wt % CpPOSS was fluidlike at low frequencies. Considered together with the T_g behavior discussed in reference to Figure 2, we postulate that observed nonterminal behavior for CpPOSS and CyPOSS copolymers is due to intermolecular POSS−PS segment interactions, following the sequence of increasing strength: ^{i}BuPOSS < CpPOSS < CyPOSS.

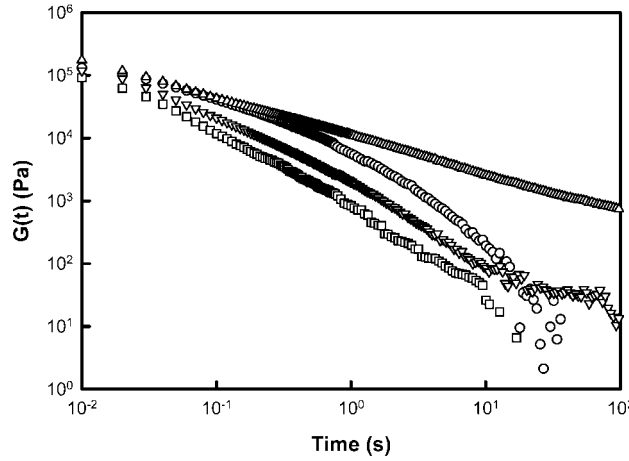

Figure 6. Shear relaxation modulus, $G(t)$, for as-cast films of the random copolymers with 15 wt % POSS as a function of vertex group: (○) PS; (□) ^{i}BuPOSS, (△) CpPOSS, and (▽) CyPOSS with step shear strain of 5% at 170 °C.

In order to further understand the effect of vertex groups on the terminal behavior, we conducted the stress relaxation experiments, where shear stress is monitored following application of a small (linear) and near-instantaneous shear strain, γ_0, to yield $G(t) = \sigma(t)/\gamma_0$. Figure 6 shows the stress relaxation curves of random copolymers with 15 wt % POSS loading and different vertex groups at 170 °C. The random copolymer with 15 wt % ^{i}BuPOSS has stress relaxation behavior quite similar to pure PS, while CpPOSS and CyPOSS copolymers feature unique behavior. Consistent with our assertion of critical gel behavior on the basis of dynamic oscillation data, $PS_{85}CpPOSS_{15}$ reveals a relaxation modulus following power law decay. This unique relaxation behavior is closely related to "gel point" with self-similar structures.

Winter et al.[40] suggested that when the polymer system is at the critical condition from meltlike to solidlike, the relaxation modulus could be expressed as follows:

$$G(t) = S_c t^{-n_c} \qquad \text{for } t > \lambda_0 \quad (6)$$

where S_c is the gel stiffness, n_c is the critical relaxation exponent, and λ_0 is the relaxation time denoting the crossover to some faster dynamics, such as segmental dynamics. For the $PS_{85}CpPOSS_{15}$, the gel stiffness, S_c, and the critical relaxation exponent, n_c, were measured to be 10^4 Pa and 0.61, respectively. By comparison, the analogous CyPOSS copolymer, $PS_{85}CyPOSS_{15}$, displayed complex behavior, the relaxation first hesitating after ca. 10 s at a stress plateau of 60 Pa, followed by continued relaxation (as a fluid) after a total delay of around 80 s. The intermediate plateau observed is consistent with that seen in oscillatory shear, shown in Figure 4. Additionally, its shear modulus begins relaxing after a characteristic time of about 80 s with a slope close to 2, although the data are too noisy to accurately measure the slope within the limited data at long times.

Finally, we were interested in comparing the effect of vertex groups on terminal relaxation behavior. Experimentally, there are several methods to obtain terminal relaxation times for linear polymers. In the framework of the tube model, the relaxation

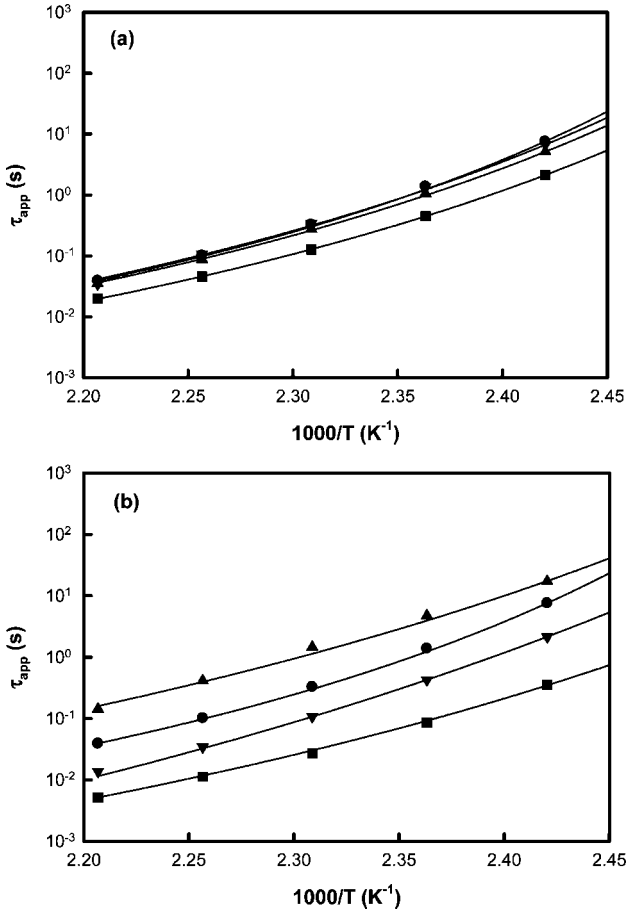

Figure 7. Temperature dependence of apparent terminal relaxation time (τ) for as-cast films of random copolymers as a function of vertex group with (a) 6 wt % and (b) 15 wt % POSS: (●) PS; (■) ^{i}BuPOSS, (▲) CpPOSS, and (▼) CyPOSS. The solid lines represent the best-fit VFTH curves for the copolymers and PS homopolymer.

of polymer chains in the terminal zone follows the configurational rearrangement accomplished by reptation-like diffusion along its contour with a random choice of new paths. The resulting terminal relaxation time predicted by this model can be expressed as[33]

$$\tau \equiv \eta_0 J_e^0 = \frac{12\eta_0}{\pi^2 G_N^0} \tag{7}$$

For the present study, however, we were unable to obtain zero shear viscosity values due to the lack of a clear terminal zone, discussed above, particularly for random copolymers incorporating CyPOSS and CpPOSS. To proceed, we employed the reciprocal crossover frequency (ω_c) (where $G_c(\omega_c) = G'(\omega_c) = G''(\omega_c)$) in approximating the terminal relaxation time using the expression $\tau_{app} \cong \omega_c^{-1}$, and such data are plotted in Figure 7. Further complicating matters, τ_{app} is a function of molecular weight, not held constant in our study due to utilization of free radical polymerization. As such, the terminal relaxation time data exhibit complex dependence on POSS content, vertex group, and polymerization degree (Figure 5a,b).

Despite this complexity, we can extract the impact of POSS on terminal relaxation behavior by focusing on its temperature dependence. Generally, the temperature dependence of terminal relaxation time within the range of $T_g < T < T_g + 100$ K can be well-described by the Vogel−Fulcher−Tamman−Hesse (VFTH) equation:[42−44]

$$\tau_{app} = \tau_\infty \exp\left(\frac{B}{T - T_0}\right) \tag{8}$$

where τ_∞ is a short reference time scale (like a hopping time), T_0 is the so-called "ideal glass transition temperature", and B is referred to as the "apparent activation energy", physically representing an Arrhenius-like temperature activation energy (though with units of temperature). The ideal glass transition temperature, also known as the Vogel temperature, is less than the T_g measured by DSC and can be computed as $T_0 = T_r - C_2$,[35] with T_r and C_2 defined earlier in the context of tTS. By best-fitting VFTH equation, with T_0 constrained by C_2 measurements and with the temperature dependence of terminal relaxation time of random copolymers incorporating 6 and 15 wt % POSS (Figure 7), we obtained the VFTH parameters as a function of POSS content and vertex group. Figure 8 shows the apparent activation energy, B, increases with increasing POSS content, regardless of vertex group. The copolymerization with POSS groups lowers the temperature dependence of polymer chain relaxation. Meanwhile, the apparent activation energy also features strong vertex group dependence: ^{i}BuPOSS < CpPOSS < CyPOSS, at least for the 15 wt % case. Thus, we observed the lowering of the temperature sensitivity for apparent terminal relaxation times due to POSS incorporation and additional sensitivity to vertex group composition, consistent with α_f measurements within the WLF model, discussed earlier.

Discussion

Architecturally, POSS groups grafted on the PS chain can be considered compact, short-chain branches that alter the chain topology and introduce additional free volume.[5] Additionally, if we regard the POSS molecule as a functional group, the presence of POSS results in additional intermolecular interactions between POSS−POSS and/or POSS−PS matrix. The analysis of WLF equation and the terminal rheological behavior of the random copolymers confirmed these two categories of effects, respectively.

The rubbery plateau modulus is related to the effect of POSS group on the microscopic topology of polymer chain and intermolecular interaction. It was argued, within the framework of the reptation tube theory, that the presence of POSS molecules significantly changes the microscopic topology of the random copolymer chains and leads to an increase in the effective tube diameter.[5] It could be the origin of POSS-based dilution of entanglement density and the decrease of the resulting rubbery plateau modulus. If there is the strong intermolecular interaction, the plateau modulus will be enhanced, and there will be two characteristic relaxation times above glass transition temperature (T_g): one for disentanglement and the other for disassociation of specific intermolecular interactions. In this study, we observed that the rubbery plateau moduli for CpPOSS and CyPOSS copolymers *decreased* with the increasing POSS loading, while their DSC data and terminal relaxation behaviors showed evidence for significant intermolecular interactions. Furthermore, the vertex group dependence of rubbery plateau modulus follows the sequence CyPOSS < CpPOSS < ^{i}BuPOSS. This trend is opposite expectations based on intermolecular interactions between POSS and PS host, suggesting that microscopic topology of polymer chains plays a dominant role in the rubbery plateau modulus when POSS loading is ≤15 wt %.

Since their sizes are comparable to a polymeric coil, pendent POSS groups grafted on the PS chain play the same role as branches. There are a few studies on the melt rheology reported for branched polystyrene.[45−48] Ferri et al.[45] studied the melt rheology of linear and randomly branched polystyrene (LPS and RBPS). They found that the shift factors (a_T) of LPS are not very different from those of RBPS. Meanwhile, the activation

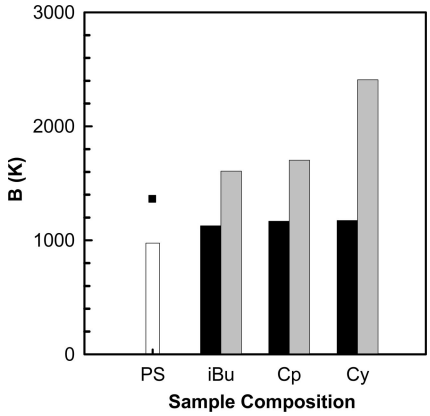

Figure 8. Best-fit apparent activation energy, *B*, of VFTH curves for PS-based random copolymers incorporating POSS moieties with different POSS vertex groups: 6 wt % (black bars) and 15 wt % (gray bars) POSS content. The square datum point stands for the value reported previously for PS (1361 K).[45]

energy was observed to slightly increase with the branching degree, demonstrating a weaker temperature dependence of terminal relaxation for RBPS than for LPS. Our results revealed increasing activation energy with POSS incorporation (POSS branching) consistent with those observed in the randomly branched polystyrene.[45] There are several theoretical models to explain the effects of branches on the temperature dependence of terminal relaxation time, including coupling models[49−51] and the reptation theory.[52] Their predictions are consistent with our observations in the random copolymers of styrene with styryl-POSS, although they are applicable to the polymers with polymeric coil branches. This consistency may stem from the nature of the POSS branches, well-defined nanoscale cage, pendent to the polymer main chain.

Additionally, Romo-Uribe et al.[4] noticed a 10-fold linear density (mass/backbone length) difference between styryl-POSS and 4-methylstyrene. The massive POSS elements, like non-diffusive "anchors", were suggested to play a large inertial effect and dramatically alter dynamics of the whole polymer chain, speculation later substantiated by molecular dynamics (MD) simulations of Bharadwaj et al.[10] on POSS−polynorbornene (PN) random copolymers. Moreover, the MD simulations indicated that CpPOSS−PN and CyPOSS−PN copolymers showed weaker temperature dependence of elastic moduli than pure PN, in accordance with the present report. Still further, Bharadwaj et al.[10] reported volumetric thermal expansion coefficients for POSS−PN copolymer melts with 10 wt % loading: $PN_{90}CpPOSS_{10}$ (6.49×10^{-4} K^{-1}) > $PN_{90}CyPOSS_{10}$ (5.20×10^{-4} K^{-1}). This vertex group dependence is in accord with our observations in tTS analysis although they did not provide the corresponding value of iBuPOSS counterpart.

Conclusions

We investigated the thermal and linear rheological behavior of polystyrene (PS)-based random copolymers incorporating POSS with three kinds of vertex groups: isobutyl (^{i}Bu), cyclopentyl (Cp), and cyclohexyl (Cy). The weak iBuPOSS−PS segment interaction resulted in a glass transition temperature (T_g) that monotonically decreased with increasing ^{i}BuPOSS content. Conversely, the strong CpPOSS/CyPOSS−PS segment interaction resulted in glass transition enhancement, though with complex dependence in the CyPOSS case. We assert that the vertex group dependence of the glass transition of the copolymers results from competing effects of free volume addition and intermolecular interactions.

Up to 15 wt % POSS loading, rheological characterization showed that time−temperature superposition (tTS) works well over the range of temperatures and POSS contents explored. The well-fitted WLF equation revealed the vertex group dependence of the corresponding thermal expansivity of free volume (α_f) follows the sequence CyPOSS < CpPOSS < ^{i}BuPOSS, and the values of α_f decrease with the increasing POSS contents. It was argued, within the framework of the reptation tube theory, that the presence of a POSS moiety significantly changes the microscopic topology of the random copolymer chains and leads to an increase in the effective tube diameter, which could be the origin of POSS-based dilution of entanglement density. The vertex group effect only plays a minor role in the rubbery plateau. More specifically, the rubbery plateau modulus decreased with increasing POSS content and in proportion to the POSS size, following the sequence ^{i}BuPOSS > CpPOSS > CyPOSS.

The strong interactions between CpPOSS/CyPOSS and PS matrix dramatically altered terminal zone response. In contrast, ^{i}BuPOSS copolymers and PS homopolymer featured a monotonic increase of tan δ with the decreasing reduced frequency; the 15 wt % CpPOSS copolymer revealed near frequency-independence tan δ at the terminal zone, characteristic of a "critical gel" formed by the strong interactions between CpPOSS−PS segments. The loss tangent, tan δ, master curves of random copolymers with 6 and 15 wt % CyPOSS featured an additional relaxation peak at the terminal zone, also attributed to strong intermolecular interactions between CyPOSS and PS matrix. The apparent terminal relaxation times, estimated by the crossover frequency, were found to be less sensitive to the temperature change for POSS copolymers than for the pure linear PS. Regardless of vertex group, the apparent activation energy of the POSS copolymers increased with the increasing POSS loading. Meanwhile, it also features a strong vertex group dependence: ^{i}BuPOSS < CpPOSS < CyPOSS.

Supporting Information Available: Figures showing (1) ^{1}H NMR spectra of POSS−styrene monomer and $PS_{70}CyPOSS_{30}$ copolymer, (2) raw differential scanning calorimetry (DSC) traces, (3) WLF function plots, (4) computed fractional free volume temperature dependences, and (5) Han plot of rheological data. This material is available free of charge via the Internet at http://pubs.acs.org.

References and Notes

(1) Ray, S. S.; Okamoto, M. *Prog. Polym. Sci.* **2003**, *28*, 1539–1641.
(2) Thostenson, E. T.; Ren, Z.; Chou, T. W. *Compos. Sci. Technol.* **2001**, *61*, 1899–1912.
(3) Huang, Z. M.; Zhang, Y. Z.; Kotaki, M.; Ramakrishna, S. *Compos. Sci. Technol.* **2003**, *63*, 2223–2253.
(4) Romo-Uribe, A.; Mather, P. T.; Haddad, T. S.; Lichtenhan, J. D. *J. Polym. Sci., Part B: Polym. Phys.* **1998**, *36*, 1857–1872.
(5) Wu, J.; Haddad, T. S.; Kim, G.-M.; Mather, P. T. *Macromolecules* **2007**, *40*, 544–554.
(6) Kopesky, E. T.; Haddad, T. S.; Cohen, R. E.; McKinley, G. H. *Macromolecules* **2004**, *37*, 8992–9004.
(7) Madbouly, S. A.; Otaigbe, J. U.; Nanda, A. K.; Wicks, D. A. *Macromolecules* **2007**, *40*, 4982–4991.
(8) Kim, B.-S.; Mather, P. T. *Macromolecules* **2002**, *35*, 8378–8384.
(9) Zheng, L.; Hong, S.; Cardoen, G.; Burgaz, E.; Gido, S. P.; Coughlin, E. B. *Macromolecules* **2004**, *37*, 8606–8611.
(10) Bharadwaj, R. K.; Berry, R. J.; Farmer, B. L. *Polymer* **2000**, *41*, 7209–7221.
(11) Leibler, L.; Rubinstein, M.; Colby, R. H. *Macromolecules* **1991**, *24*, 4701–4707.
(12) Stadler, R.; De lucca Freitas, L. L. *Colloid Polym. Sci.* **1986**, *264*, 773–778.
(13) De lucca Freitas, L. L.; Stadler, R. *Macromolecules* **1987**, *20*, 2478–2485.
(14) Shaw, M. T.; MacKnight, W. J. *Introduction to Polymer Viscoelasticity*, 3rd ed.; John Wiley & Sons: Hoboken, NJ, 2005.
(15) Moore, B. M.; Haddad, T. S.; Gonzalez, R. I. *Polym. Prepr. (Am. Chem. Soc., Div. Polym. Chem.)* **2004**, *45*, 692–693.

(16) Moore, B. M.; Haddad, T. S.; Gonzalez, R. I.; Schlaefer, C. *Polym. Prepr. (Am. Chem. Soc., Div. Polym. Chem.)* **2004**, *45*, 692–693.
(17) Atkins, E. D. T.; Isaac, D. H.; Keller, A.; Miyasaka, K. *J. Polym. Sci., Polym. Phys. Ed.* **1977**, *15*, 211–226.
(18) Mitchell, G. R.; Windle, A. H. *Polymer* **1984**, *25*, 906–920.
(19) Zhang, W.; Fu, B. X.; Seo, Y.; Schrag, E.; Hsiao, B.; Mather, P.; Yang, N.-L.; Xu, D.; Ade, H.; Rafailovich, M.; Sokolov, J. *Macromolecules* **2002**, *35*, 8029–8038.
(20) Rogers, S.; Mandelkern, L. *J. Phys. Chem.* **1957**, *61*, 985–991.
(21) Xu, H.; Kuo, S.-W.; Lee, J.-S.; Chang, F.-C. *Polymer* **2002**, *43*, 5117–5124.
(22) Xu, H.; Kuo, S. W.; Lee, J. S.; Chang, F. C. *Macromolecules* **2002**, *35*, 8788–8793.
(23) Haddad, T. S.; Choe, E.; Lichtenhan, J. D. *Mater. Res. Soc. Symp. Proc.* **1996**, *435*, 25–32.
(24) Haddad, T. S.; Lichtenhan, J. D. *Macromolecules* **1996**, *29*, 7302–7304.
(25) Mather, P. T.; Jeon, H. G.; Romo-Uribe, A.; Haddad, T. S.; Lichtenhan, J. D. *Macromolecules* **1999**, *32*, 1194–1203.
(26) Lichtenhan, J. D.; Otonari, Y. A.; Carr, M. J. *Macromolecules* **1995**, *28*, 8435–8437.
(27) Lichtenhan, J. D.; Vu, N. Q.; Carter, J. A.; Gillman, J. W.; Feher, F. J. *Macromolecules* **1993**, *26*, 2141–2142.
(28) Onogi, S.; Masuda, T.; Kitagawa, K. *Macromolecules* **1970**, *3*, 109–116.
(29) Bharadwaj, R. K.; Berry, R. J.; Farmer, B. L. *Polymer* **2000**, *41*, 7209–7221.
(30) Bizet, S.; Galy, J.; Gérard, J.-F. *Polymer* **2006**, *47*, 8219–8227.
(31) Wu, S. *J. Polym. Sci., Part B: Polym. Phys.* **1987**, *25*, 557–566.
(32) Wu, S. *J. Polym. Sci., Part B: Polym. Phys.* **1987**, *25*, 2511–2529.
(33) Doi, M.; Edwards, S. F. *The Theory of Polymer Dynamics*; Oxford University Press: Oxford, 1986.
(34) Larson, R. G.; Sridhar, T.; Leal, L. G.; McKinley, G. H.; Likhtman, A. E.; McLeish, T. C. B. *J. Rheol.* **2003**, *47*, 809–818.
(35) Ferry, J. D. *Viscoelastic Properties of Polymers*, 3rd ed.; John Wiley & Sons: New York, 1980.
(36) Barry, A. J.; Daudt, W. H.; Domicone, J. J.; Gilkey, J. W. *J. Am. Chem. Soc.* **1955**, *77*, 4248–4252.
(37) Larsson, K. *Ark. Kemi* **1960**, *16*, 203–208.
(38) Larsson, K. *Ark. Kemi* **1960**, *16*, 209–214.
(39) Höcker, H.; Blake, G. J.; Flory, P. J. *Trans. Faraday Soc.* **1971**, *67*, 2251–2257.
(40) Winter, H. H.; Chambon, F. *J. Rheol.* **1986**, *30*, 367–382.
(41) Chambon, F.; Winter, H. H. *J. Rheol.* **1987**, *31*, 683–697.
(42) Vogel, H. *Phys. Z.* **1921**, *22*, 645–646.
(43) Tamman, G.; Hesse, W. Z. *Z. Anorg. Allg. Chem.* **1926**, *156*, 245–257.
(44) Fulcher, G. S. *J. Am. Ceram. Soc.* **1925**, *8*, 339–355.
(45) Ferri, D.; Lomellini, P. *J. Rheol.* **1999**, *43*, 1355–1372.
(46) Graessley, W. W.; Roovers, J. *Macromolecules* **1979**, *12*, 959–965.
(47) Rooves, J. *Macromolecules* **1984**, *17*, 7521–7526.
(48) Masuda, T.; Ohta, Y.; Onogi, S. *Macromolecules* **1986**, *19*, 2524–2532.
(49) Bero, C. A.; Roland, C. M. *Macromolecules* **1996**, *29*, 1562–1568.
(50) Ngai, K. L.; Roland, C. M. *J. Polym. Sci., Part B: Polym. Phys.* **1997**, *35*, 2503–2510.
(51) Santangelo, P. G.; Ngai, K. L.; Roland, C. M. *Polymer* **1998**, *39*, 681–687.
(52) Graessley, W. W. *Macromolecules* **1982**, *15*, 1164–1167.

MA8024267